Materials Science Forum
ISSN: 1662-9752, Vol. 897, pp 755-758
doi:10.4028/www.scientific.net/MSF.897.755

Submitted: 2016-09-12
Revised: 2017-01-24
Accepted: 2017-01-27
Online: 2017-05-15

Bulk β-Ga_2O_3 with (010) and ($\bar{2}$01) Surface Orientation: Schottky Contacts and Point Defects

M. E. Ingebrigtsen[1,a*], L. Vines[1,b], G. Alfieri[2,c], A. Mihaila[2,d], U. Badstübner[2,e], B.G. Svensson[1,f], A. Kuznetsov[1,g]

[1]University of Oslo, Pb 1048 Blindern, 0316 Oslo, Norway

[2]ABB Corporate Research, Segelhofstrasse 1K, 5405 Baden-Dättwil, Switzerland

[a]m.e.ingebrigtsen@smn.uio.no, [b]lasse.vines@fys.uio.no, [c] giovanni.alfieri@ch.abb.com, [d]andrei.mihaila@ch.abb.com, uwe.badstuebner@ch.abb.com, [e]b.g.svensson@fys.uio.no, [f]andrej.kuznetsov@fys.uio.no

Keywords: Schottky contacts, defects, β-Ga_2O_3, deep level transient spectroscopy, current-voltage, thermal admittance spectroscopy, secondary ion mas spectrometry.

Abstract. Electrical properties of Schottky contacts of high work-function metals (Pd, Au, and Ni) on (010) and ($\bar{2}$01) oriented β-Ga_2O_3 were investigated. Current-voltage characteristics reveal that all the contacts exhibit high rectifying behavior with ideality factors as low as 1.04. However, the reverse leakage currents were lower in the (010) samples compared to the ($\bar{2}$01) ones. Thermal admittance spectroscopy confirms a main charge carrier level to be at ~15 meV below the conduction band edge (E_c). Secondary ion mass spectrometry indicates that Si may be responsible for this donor level. Deep level transient spectroscopy reveals four levels (E1-E4) in the upper part of the band gap, with the corresponding energy level positions at 0.56, 0.76, 1.01, and 1.48 eV below E_c.

Introduction

Gallium oxide (Ga_2O_3) is attracting increased attention due to its potential applications in UV detectors and high voltage diodes [1]. Ga_2O_3 can be found in several crystalline modifications, where β-Ga_2O_3 is the most stable phase at ambient conditions. β-Ga_2O_3 exhibits a monoclinic crystal structure and a wide energy bandgap of ~4.7 eV [2]. An important characteristic of β-Ga_2O_3 is the high breakdown field, estimated at ~8 MV/cm [3], making it a promising candidate for use in power electronics. Recent advances in the β-Ga_2O_3 synthesis have lifted its bulk crystal quality, particularly using melt growth methods, including so called Edge-defined Film-fed Growth (EFG) [4].

Controlling charge carrier concentrations is essential in device fabrication, and n-type β-Ga_2O_3 with electron concentrations in the range of 10^{16} to 10^{19} cm^{-3} is readily achievable by doping with, e.g., Sn [3]. While the oxygen vacancy (V_O) was previously considered as a candidate for the origin of the native n-type conductivity in β-Ga_2O_3, recent density functional calculations indicate that V_O is a deep donor not being ionized at room temperature [5]. An alternative explanation of the native conductivity may be given in terms of unintentional extrinsic impurities like Si and H. However, as with most semiconducting oxides, p-type conductivity in β-Ga_2O_3 is challenging. Acceptor levels can be induced by Fe and Mn, but their deep energy positions cause compensation of the native n-type conductivity rather than to provide p-type conductivity [6, 7]. Deep level transient spectroscopy (DLTS) has revealed three electronic states in the upper part of the band gap [8], but their origin is not established. As such, the understanding of both intrinsic and impurity related defects in β-Ga_2O_3 has to be improved.

Further, to produce high performance devices, achieving well controlled rectifying junctions is a prerequisite. Accounting for the lack of p-type β-Ga_2O_3, such junctions are only achieved with Schottky contacts. Metals with high work functions are needed for this purpose, and reports in literature suggest good ideality factors and high energy barriers for β-Ga_2O_3 Schottky diodes using Au, Ni, Pt and Cu [8-11].

The present contribution deals with β-Ga_2O_3 synthesized via the EFG method and cut along different orientations. Herein, we report a systematic investigation of Schottky diode characteristics, revealing prominent electronic states, and make an effort for defect identification in β-Ga_2O_3.

Experimental

We have investigated single crystalline β-Ga_2O_3 wafers with surface orientations (010) and ($\bar{2}$01) produced by Tamura from EFG ingots. Samples of 5×5 mm in size were cut from 0.65 mm thick wafers of each orientation. Notably, we tested samples originated from different batches, so that different impurity backgrounds were possible to investigate too. One side, chemical mechanically polished with a roughness <0.15 nm (similar for both orientations), was used for the Schottky contact preparation (after cleaning in organic solvents (acetone and isopropanol) and rinsing in de-ionized water) using electron-beam evaporation of Pd and Ni, and thermal evaporation of Au, through a shadow mask. All the metals are anticipated to exhibit high barrier heights (ϕ_B) according to the Schottky-Mott model. Backside ohmic contacts were deposited using electron-beam deposition of Ti (10 nm) and Al (100 nm), where the ohmic behavior was confirmed by transmission-line measurements on similar samples. Electrical characterization was done with current-voltage (IV), capacitance-voltage (CV), DLTS, and thermal admittance spectroscopy (TAS). For the spectroscopic techniques, two different setups were used, covering the temperature range of 20 – 680 K. DLTS was performed with a -8 V reverse bias voltage and pulsing to -1 V, thus probing from ~80 nm from the Schottky contact interface and into the bulk of the β-Ga_2O_3 substrates. Six rate windows were used to record the capacitance transients, and the signal was processed with a lock-in weighting function to extract the DLTS spectra. Secondary ion mass spectrometry (SIMS) was used to study residual impurities in the samples, and the concentration calibration was done by comparison with implanted reference samples.

Results

Fig. 1 shows the IV characteristics of selected contacts on samples with (010) and ($\bar{2}$01) surface orientation. Highly rectifying junctions are demonstrated for all metals used, e.g. more than eight orders of magnitude of rectification are obtained for Ni on the (010) surface. The reverse leakage current is close or below the detection limit of the measurement setup for the (010) samples. Further, the (010) samples with Pd and Ni contacts reveal ideality factors (n) close to unity. Taking into account image-force lowering, the contacts can be assumed to be dominated by thermionic emission across the barrier. For Au, a lower rectification and higher ideality factor is observed, which may be related to a lower adhesion of Au to β-Ga_2O_3. In addition, some contacts show a shift in forward bias, possibly indicating the formation of an insulating interfacial layer. The Schottky contacts on ($\bar{2}$01) substrates exhibit significantly higher ideality factors, and also the typical reverse leakage current is higher, at least for Pd and Ni compared to their counterparts on the (010) substrates. This trend indicates a lower interface quality of the Shottky contacts depending on the β-Ga_2O_3 orientation, as no significant dependence on carrier concentration is observed. Ideality factors and barrier heights, as derived from the forward IV characteristics[12], for the contacts in Fig. 1 are summarized in Table 1.

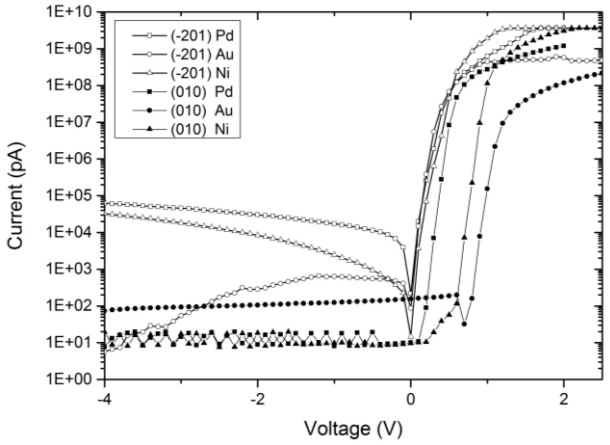

Figure 1 – IV characteristics of Schottky contacts as manufactured on (010) and ($\bar{2}$01) oriented β-Ga_2O_3, as labelled with filled and open symbols, respectively.

CV measurements, with a 1 MHz probing frequency, reveal carrier concentrations in the range 0.6-1.8×10^{17} and 1.3-3.2 ×10^{17} cm^{-3} for the (010) and ($\bar{2}$01) samples, respectively, with

Table 1 – Barrier heights and ideality factors for Au, Pd, and Ni Schottky contacts $_3$ on (010) and ($\bar{2}$01) β-Ga_2O_3.

	(010) β-Ga_2O_3			($\bar{2}$01) β-Ga_2O_3		
	Au	Pd	Ni	Au	Pd	Ni
ϕ_B [eV]	1.45	1.01	1.37	1.34	1.29	1.30
n	1.25	1.04	1.05	1.33	1.76	1.72

the distribution being present as lateral inhomogeneity over the wafer. The observed concentration range is close to the specifications from Tamura. TAS spectra reveal one-step freeze out of the charge carriers at ~30 K for measurement frequencies between 10 kHz and 1 MHz, see Fig. 2 showing selected data. The single freeze-out corresponds to a shallow level at $\Delta H = 15 \pm 8\ meV$ below the conduction band, independently of the surface orientation. Interestingly, while not intentionally doped, SIMS reveal the presence of Si, Al and In at concentrations above 1×10^{17} cm^{-3}, i.e. similar or above the electron concentration. Among these three, Si is expected to be a shallow donor [5] and is a likely candidate for the n-type behavior in our samples.

Using DLTS, four deep levels with energy positions at 0.56, 0.76, 1.01, and 1.48 eV below E_c were observed and labelled as E1-E4, respectively. The E1-E3 levels correspond well with those reported by Irmscher et al. [8], while the deeper E4 has not been reported previously. Table 2 lists the energy positions (E_t) and the apparent electron capture cross section (σ_n) of the observed levels. The values are extracted from measurements on several samples and the intervals represent the spread in data between the samples. Fig. 3 compares the DLTS spectra obtained from the samples with different surface orientations employing Au and Ni Schottky contacts. Here, the concentration of the deep levels is related to the amplitude of the DLTS signatures by $N_t = 2N_d * \Delta C/C$, with N_d being the charge carrier concentration as found from the CV measurements. Notably, the E2 concentration in the ($\bar{2}$01) samples is considerably higher compared to that in the (010) samples. In contrast, the E1 level is more prominent in the (010) samples, albeit with a much lower intensity than E2 in the ($\bar{2}$01) samples. One potential explanation of this observation may be associated with the difference in band bending occurring at the two β-Ga_2O_3 surfaces and hence Fermi level position relative to E_C. This effect may in particular influence the balance of the intrinsic point defects in the vicinity of the interface, and be detected in the DLTS spectra. However, in addition to the interface and intrinsic defects being responsible for the E1-E4 signatures in Fig.3, impurities may play a role too. Indeed, several impurities are present in the 10^{15}-10^{16} cm^{-3} range, as measured by SIMS, including Mg, Cr, Fe and Ni. Interestingly, some variations in the impurity content is detected for different sample orientations, and the most pronounced difference occurs for Fe, with concentrations of ~4×10^{17} and 7×10^{16} cm^{-3} in the ($\bar{2}$01) and (010) samples, respectively. This difference may perhaps be attributed to variations over different batches of the EFG synthesis,

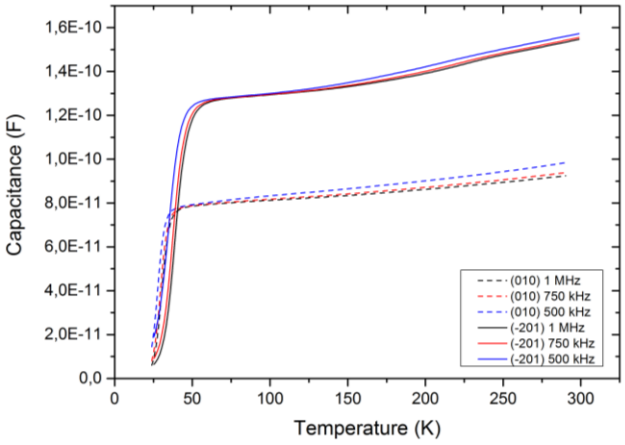

Figure 2 – Typical TAS spectra, i.e. capacitance as function of temperature at different probing frequencies, for (010) and ($\bar{2}$01) samples with Ni contacts. A dominant level occurs at ~15 meV below the conduction band edge.

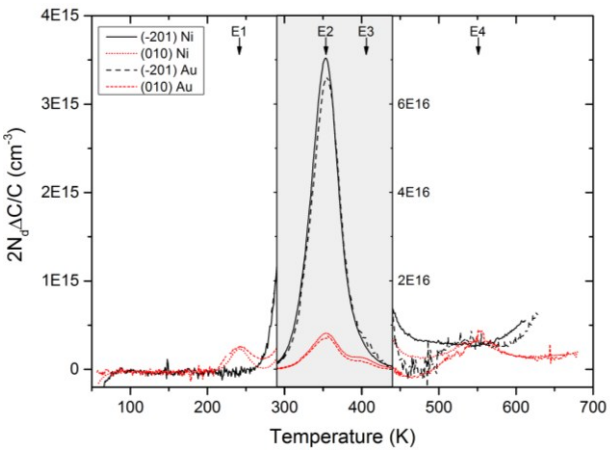

Figure 3 – A comparison of the defect concentrations of samples with Au and Ni Schottky contacts on (010) and ($\bar{2}$01) oriented β-Ga_2O_3. Note the different concentration scales for E1/E4 and E2/E3.

Table 2 – Energy positions (E_t) bellow E_C and apparent capture cross sections (σ_n) for deep levels observed in β-Ga_2O_3 using Ni Schottky contacts on (010) substrates.

	E1	E2	E3	E4
$E_t\ [eV]$	0.56 ± 0.03	0.76 ± 0.03	1.01 ± 0.05	1.48 ± 0.05
$\sigma_n\ [cm^2]$	$0.3 - 5 * 10^{-13}$	$0.6 - 1.1 * 10^{-15}$	$0.2 - 4 * 10^{-13}$	$0.8 - 6 * 10^{-13}$

rather than being caused by the surface orientation. Accordingly, different impurity backgrounds may also explain the difference in the deep level concentrations as observed by DLTS. Notably, the factor ~6 difference in the Fe concentration as deduced from SIMS is close to the ratio in the E2 intensities between the $(\bar{2}01)$ and (010) substrates, as seen from Fig. 3. However, the absolute concentration of Fe observed by SIMS is higher than E2, but may be attributed to Fe existing in different configurations in the material, similar to the Fe-related E2 level observed in ZnO [13]. Further investigations are necessary to proceed with detailed identification of the deep levels.

Concluding remarks

We have shown that high quality Schottky contacts are accomplished on β-Ga_2O_3 using several metals, and this holds in particular for wafers with (010) surface orientation. Ni is revealed as an inexpensive and better alternative to Au providing more robust contacts. Combining TAS and SIMS, Si is proposed to be a main donor, with ionization energy of ~15 meV. Further, four deep levels (E1-E4) were detected by DLTS. E1-E3 were reported previously in the literature, while E4, which is situated deep in the band gap, is reported for the first time. The difference in the surface charges as well as variations in the extrinsic impurity contents, particularly of Fe, were discussed to explain the trend in the E1 and E2 intensities revealed by DLTS.

Acknowledgements

Financial support is acknowledged from the Research Council of Norway through the MIDAS (Project No. 228578) and Salient (Project No. 239895) projects.

References

[1] Higashiwaki, M., K. Sasaki, H. Murakami, Y. Kumagai, A. Koukitu, A. Kuramata, T. Masui, S. Yamakoshi. Semicond. Sci. Technol., 31 (2016): p. 034001.
[2] Tippins, H.H. Phys. Rev., 140 (1965): p. A316-A319.
[3] Sasaki, K., A. Kuramata, T. Masui, E.G. Víllora, K. Shimamura, S. Yamakoshi. Appl. Phys. Express, 5 (2012): p. 035502.
[4] Aida, H., K. Nishiguchi, H. Takeda, N. Aota, K. Sunakawa, Y. Yaguchi. Jpn. J. Appl. Phys., 47 (2008): p. 8506.
[5] Varley, J.B., J.R. Weber, A. Janotti, C.G. Van de Walle. Appl. Phys. Lett., 97 (2010): p. 142106.
[6] Higashiwaki, M., K. Sasaki, T. Kamimura, M. Hoi Wong, D. Krishnamurthy, A. Kuramata, T. Masui, S. Yamakoshi. Appl. Phys. Lett., 103 (2013): p. 123511.
[7] Guo, D., P. Li, Z. Wu, W. Cui, X. Zhao, M. Lei, L. Li, W. Tang. Sci. Rep., 6 (2016): p. 24190.
[8] Irmscher, K., Z. Galazka, M. Pietsch, R. Uecker, R. Fornari. J. Appl. Phys., 110 (2011): p. 063720.
[9] Suzuki, R., S. Nakagomi, Y. Kokubun, N. Arai, S. Ohira. Appl. Phys. Lett., 94 (2009): p. 222102.
[10] Sasaki, K., M. Higashiwaki, A. Kuramata, T. Masui, S. Yamakoshi. Electron Device Letters, IEEE, 34 (2013): p. 493-495.
[11] Splith, D., S. Müller, F. Schmidt, H. von Wenckstern, J.J. van Rensburg, W.E. Meyer, M. Grundmann. Phys. Status Solidi A, 211 (2014): p. 40-47.
[12] Quemener, V., M. Alnes, L. Vines, P. Rauwel, O. Nilsen, H. Fjellvåg, E.V. Monakhov, B.G. Svensson. J. Phys. D: Appl. Phys., 45 (2012): p. 315101.
[13] Quemener, V., L. Vines, E.V. Monakhov, B.G. Svensson. Appl. Phys. Lett., 102 (2013): p.232102.